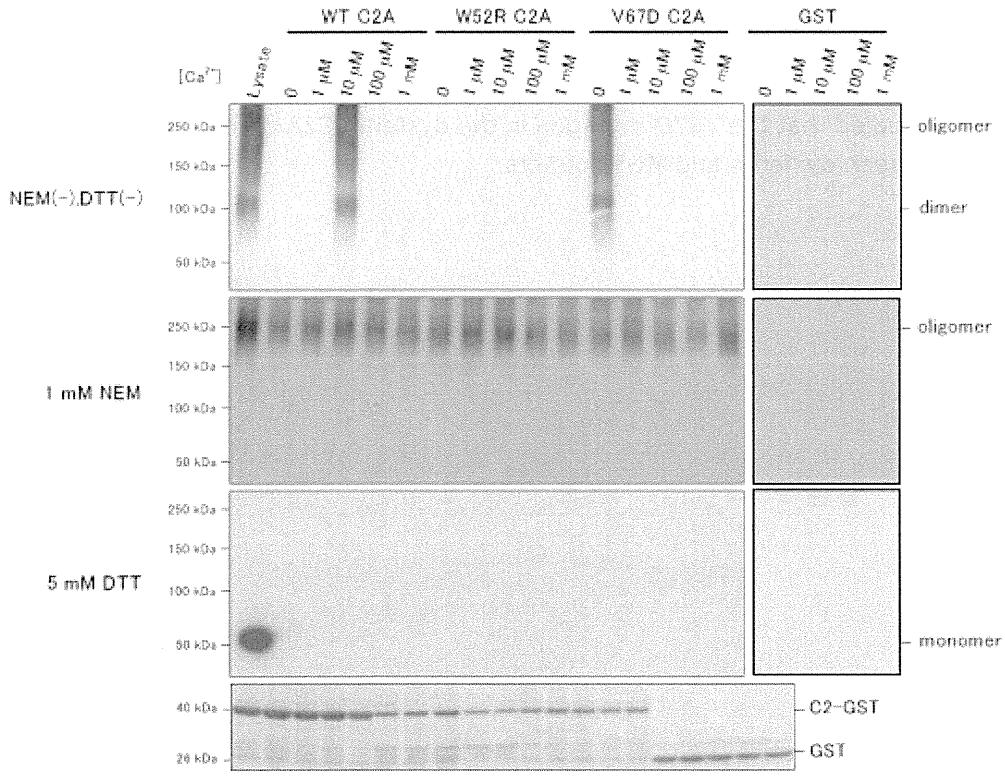

Fig. 3: Pull-down assay of dysferlin C2A-GST and MG53.

COS-7 cells overexpressing FLAG-tagged MG53 were lysed and supplemented with DTT or NEM, and proteins in these lysates were cross-linked with GA. Cross-linked proteins were incubated with glutathione Sepharose 4B beads bound to wild-type C2A-GST, V67D C2A-GST, or GST. GST fusion proteins bound to beads were separated by SDS-PAGE, followed by Coomassie Brilliant Blue R-250-staining. Precipitated MG53 oligomers/monomers were detected on immunoblots using an anti-FLAG antibody. Mutations in the C2A domain affect the association of between dysferlin and MG53.

MG53 with a C242A missense mutation shows impaired accumulation at wound sites and attenuates the formation of dysferlin patches

To examine the biological role of the association between dysferlin and MG53 in sarcolemmal repair, we used mouse skeletal muscle co-transfected with dysferlin-EGFP and RFP-tagged wild-type MG53 or RFP-tagged mutant MG53 to perform a membrane repair assay. The mutant MG53 carried a C242A missense mutation and is designated RFP-C242A-MG53 here. MG53 with a C242A missense mutation reportedly exists as a monomer or dimer when expressed in mammalian cells, but does not form oligomers via disulfide bonding [4,6]. RFP-C242A-MG53 did not accumulate at wound sites as reported previously, and it was associated with defective sarcolemmal repair [4]. Co-expression of RFP-C242A-MG53 did not affect the subcellular localization of dysferlin in myofibers, and dysferlin was localized in a striated pattern (Fig. 4A). However, RFP-C242A-MG53 compromised the accumulation of dysferlin at injury sites (Fig. 4A, B). When the movement of dysferlin and wild-type MG53 were observed simultaneously in mouse skeletal muscle, RFP-wild-type MG53 accumulated more slowly at injury sites than dysferlin-EGFP (Fig. 4A). Accumulation of dysferlin-EGFP at wound sites stops within 5 seconds of injury and disperses gradually, while wild-type MG53 continues to accumulate for 200 seconds after injury (Fig. 4A and 4B).

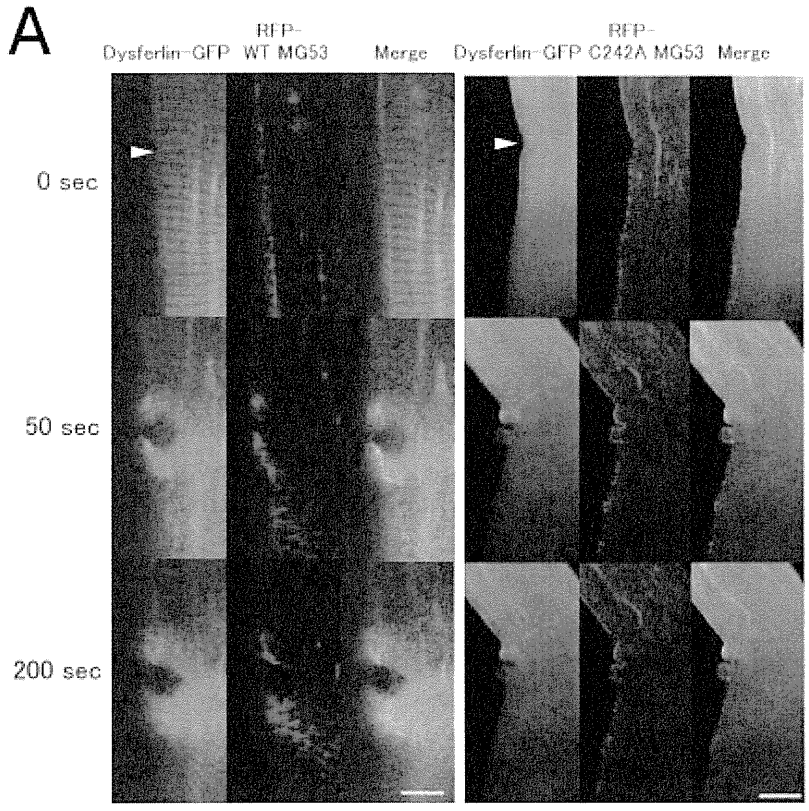
A
RFP-
Dysferlin-GFP WT MG53
Merge
RFP-
Dysferlin-GFP C242A MG53
Merge
0 sec
50 sec
200 sec

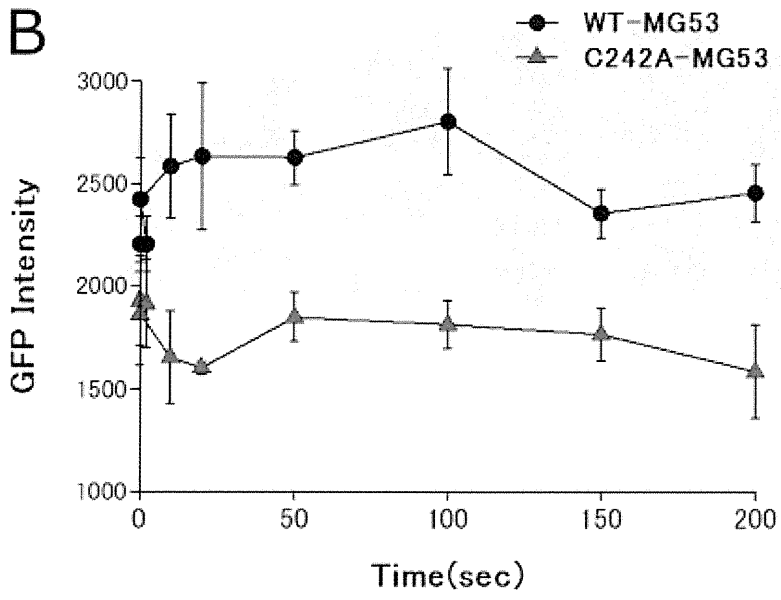

Fig. 4: Membrane repair assay of myofiber transfected with dysferlin-GFP and RFP-MG53.

RFP-C242A MG53 perturbed the accumulation of dysferlin at wound sites in the sarcolemma. A. Dysferlin-GFP was simultaneously expressed with RFP-tagged wild-type MG53 or the RFP-C242A-MG53 mutant in mouse skeletal muscle. Arrowheads indicate sites of membrane injury, which were induced with a two-photon laser microscope. Dysferlin-GFP accumulated at the injury site in the presence of RFP-wild-type MG53, but no obvious accumulation of dysferlin-GFP was observed in the presence of the RFP-C242A-MG53 mutant. Scale bar, 10 mm. B.Time course fluorescence intensity (n=3) at wounded sites versus time. For every image taken, the fluorescence intensity of dysferlin-GFP at the site of the damage (circle of 5 mm in diameter) was measured with Zeiss LSM5 Image Examinar software. Data are means ± standard deviation.

MG53 accumulates normally at injury site of sarcolemma in dysferlin-deficient mice.

A previous study revealed that exogenous expression of MG53 in undifferentiated C2C12 cells was necessary for recruitment of GFP-dysferlin to sites of injury [5]. Conversely, to examine whether the recruitment of MG53 requires dysferlin, and to elucidate the molecular pathology of dysferlinopathy, we used skeletal muscle from dysferlin-deficient A/J mice transfected with EGFP-MG53 to perform a membrane repair assay. We confirmed that EGFP-MG53 accumulated at sites of injury (Fig. 5). Sarcolemmal repair was observed and confirmed by FM4-46-loading in A/J mice (data not shown). The accumulation of MG53 at the sarcolemmal wound was observed in A/L mice, similar to wild-type mice. Similar results were obtained from the membrane repair assay using dysferlin-deficient SJL mice.

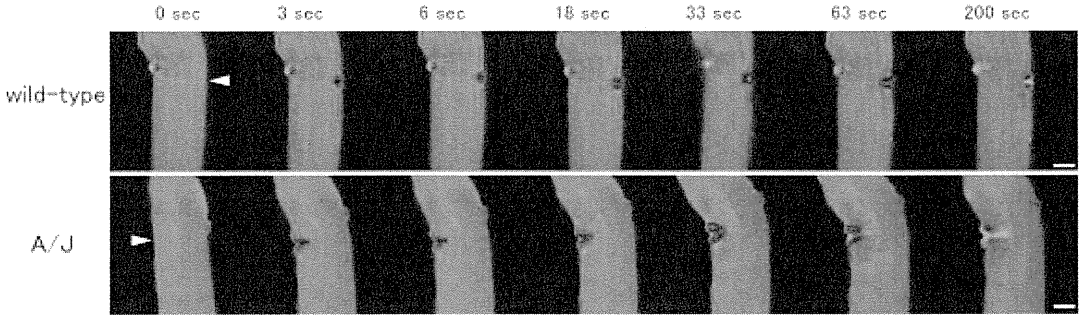

Fig. 5: Membrane repair assay of myofiber using dysferlin-deficient myofiber transfected with GFP-MG53.

GFP-MG53 accumulated at sites of injury in the sarcolemma in dysferlin-deficient A/J mice, similar to wild-type mice. GFP-MG53 was expressed in wild-type or dysferlin-deficient A/J mice, and a membrane repair assay was performed using transfected myofibers. Subcellular localization of GFP-MG53 was similar between wild-type and A/J mice. Arrowheads indicate membrane injury sites, which were induced with a two-photon laser microscope. Scale bar, 10 μm.

Discussion

Both dysferlin and MG53 are involved in membrane repair after injury in skeletal muscle. Dysferlin accumulates at wounded sarcolemmal sites, and this accumulation requires the influx of Ca^{2+} into the myofiber [3]. MG53 forms oligomers at the sarcolemmal injury site in an oxidation-dependent manner [4,6]. MG53 associates with dysferlin and facilitates vesicle trafficking to the site of membrane injury, and a recent finding suggests that MG53 and dysferlin may form a complex that participates in membrane repair in striated muscle [5]. To characterize the association between dysferlin and MG53, we used an IP assay and mouse muscle extract with or without exogenously added EGTA or $CaCl_2$ to examine the Ca^{2+} dependency of this association. Using lysis buffer that lacked EGTA and $CaCl_2$, we observed the association of dysferlin with MG53 in mouse skeletal muscle. Lysates lacking exogenously added EGTA and $CaCl_2$ contain physiological concentrations of free calcium. Hence, low concentrations of calcium are likely to be necessary for the interaction between MG53 and dysferlin.

Our results indicated that MG53 oligomers associated with the dysferlin C2A domain in the presence or absence of Ca^{2+}, whereas MG53 dimers associated with the dysferlin C2A domain in a Ca^{2+}-dependent manner. We also revealed that pathogenic mutations in the dysferlin C2A domain (W52R and V67D) alter the association between this domain and MG53 dimers in a pull-down assay. In the absence of EGTA or Ca^{2+}, dysferlin with a C2A missense mutation (W52R or V67D) did not associate with MG53 in an IP assay that used extracts from co-transfected COS-7 cells; however, full-length dysferlin with the most common pathogenic mutation found in Japan, a W999C missense mutation in the dysferlin domain, did associate with MG53 in these IP assays (data not shown). These results indicate that the dysferlin C2A domain is important for the association between dysferlin and MG53. Amino acid W52 in human dysferlin is located between the b5-sheet and the b6-sheet, and V67 is located in the b6-sheet [18]. Both residues are reportedly important for the C2 structure, particularly those of the b-sheet, and are predicted to coordinate calcium [18].

Recently, MG53 was reported to form homodimers, which are essential for MG53-mediated sarcolemmal repair [6]. We used pull-down assays to investigate associations between MG53 monomers or MG53 dimers and the

dysferlin C2A domain, and we found that MG53 dimers associated with dysferlin in a Ca^{2+}-dependent manner. An increase in the cytoplasmic Ca^{2+} level is necessary for dysferlin accumulation at wounded sarcolemmal sites [3]. The intracellular Ca^{2+} level is maintained at 50-100 nM in resting mammalian cells, but this increases to 6 μM after membrane puncture in Swiss-3T3 cells [19]. The influx of extracellular Ca^{2+} through the wound site is required for vesicle fusion with the plasma membrane and formation of a repair patch in skeletal muscle, but MG53 trafficking to the wound site does not require Ca^{2+} [4]. In pull-down assays in the present study, we demonstrated a selective association between the wild-type dysferlin C2A domain and MG53 dimers at a free Ca^{2+} concentration of 10 μM, but not at lower or higher free Ca^{2+} concentrations. These findings indicated that the concentration of free Ca^{2+} is important for association of dysferlin with MG53 dimers, and suggest that MG53 dimers not only form oligomers, but also associate with dysferlin in response to sarcolemmal injury. The altered Ca^{2+} sensitivity of the association between dysferlin with a mutation in the C2A domain and MG53 dimers in the pull-down assay also suggested that the C2A domain was important in the Ca^{2+}-dependent association between dysferlin and MG53 dimers.

We were able to analyze the movement of dysferlin and MG53 in real time during sarcolemmal repair in a membrane repair assay that employs mouse myofibers that express dysferlin-EGFP and RFP-MG53. This is the first report to demonstrate that dysferlin and MG53 have different accumulation patterns at wound sites, and this result indicated that dysferlin and MG53 have different functions in sarcolemmal repair. Our studies also revealed that MG53 carrying a C242A missense mutation can suppress the accumulation of dysferlin at the wound site; this finding, together with results from pull-down assays, suggests that MG53 dimers play an important role in sarcolemmal repair.

Our studies also revealed that MG53 accumulated at injury sites in the sarcolemma in dysferlin-deficient mice, similar to wild-type mice. However, dysferlin-deficient SJL and A/J mice have a progressive muscular dystrophy phenotype, suggesting that MG53 is necessary but not sufficient for efficient sarcolemmal repair.

Competing Interests

The authors have declared that no competing interests exist.

Correspondence

Address for correspondence : c-matsuda@aist.go.jp (C. Matsuda)

References

1. Liu J, Aoki M, Illa I, Wu C, Fardeau M, et al. (1998) Dysferlin, a novel skeletal muscle gene, is mutated in Miyoshi myopathy and limb girdle muscular dystrophy. Nat Genet 20: 31-36.

2. Bashir R, Britton S, Strachan T, Keers S, Vafiadaki E, et al. (1998) A gene related to Caenorhabditis elegans spermatogenesis factor fer-1 is mutated in limb-girdle muscular dystrophy type 2B. Nat Genet 20: 37-42.

3. Bansal D, Miyake K, Vogel SS, Groh S, Chen CC, et al. (2003) Defective membrane repair in dysferlin-deficient muscular dystrophy. Nature 423: 168-172.

4. Cai C, Masumiya H, Weisleder N, Matsuda N, Nishi M, et al. (2009) MG53 nucleates assembly of cell membrane repair machinery. Nat Cell Biol 11: 56-64.

5. Cai C, Weisleder N, Ko JK, Komazaki S, Sunada Y, et al. (2009) Membrane repair defects in muscular dystrophy are linked to altered interaction between MG53, caveolin-3 and dysferlin. J Biol Chem.

6. Hwang M, Ko JK, Weisleder N, Takeshima H, Ma J (2011) Redox-dependent oligomerization through a leucine zipper motif is essential for MG53-mediated cell membrane repair. Am J Physiol Cell Physiol 301: C106-114.

7. Tagawa K, Ogawa M, Kawabe K, Yamanaka G, Matsumura T, et al. (2003) Protein and gene analyses of dysferlinopathy in a large group of Japanese muscular dystrophy patients. J Neurol Sci 211: 23-28.

8. Ho M, Post CM, Donahue LR, Lidov HG, Bronson RT, et al. (2004) Disruption of muscle membrane and phenotype divergence in two novel mouse models of dysferlin deficiency. Hum Mol Genet 13: 1999-2010.

9. Cai C, Masumiya H, Weisleder N, Pan Z, Nishi M, et al. (2009) MG53 regulates membrane budding and exocytosis in muscle cells. J Biol Chem 284: 3314-3322.

10. Matsuda C, Kameyama K, Tagawa K, Ogawa M, Suzuki A, et al. (2005) Dysferlin interacts with affixin (beta-parvin) at the sarcolemma. J Neuropathol Exp Neurol 64: 334-340.

11. Frangioni JV, Neel BG (1993) Solubilization and purification of enzymatically active glutathione S-transferase (pGEX) fusion proteins. Anal Biochem 210: 179-187.

12. Aihara H, Miyazaki J (1998) Gene transfer into muscle by electroporation in vivo. Nat Biotechnol 16: 867-870.

13. Cho W, Stahelin RV (2006) Membrane binding and subcellular targeting of C2 domains. Biochim Biophys Acta 1761: 838-849.

14. Davis DB, Doherty KR, Delmonte AJ, McNally EM (2002) Calcium-sensitive phospholipid binding properties of normal and mutant ferlin C2 domains. J Biol Chem 277: 22883-22888.

15. Illarioshkin SN, Ivanova-Smolenskaya IA, Greenberg CR, Nylen E, Sukhorukov VS, et al. (2000) Identical dysferlin mutation in limb-girdle muscular dystrophy type 2B and distal myopathy. Neurology 55: 1931-1933.

16. De Luna N, Freixas A, Gallano P, Caselles L, Rojas-Garcia R, et al. (2007) Dysferlin expression in monocytes: a source of mRNA for mutation analysis. Neuromuscular disorders : NMD 17: 69-76.

17. Therrien C, Di Fulvio S, Pickles S, Sinnreich M (2009) Characterization of lipid binding specificities of dysferlin C2 domains reveals novel interactions with phosphoinositides. Biochemistry 48: 2377-2384.

18. Steinhardt RA, Bi G, Alderton JM (1994) Cell membrane resealing by a vesicular mechanism similar to neurotransmitter release. Science 263: 390-393.

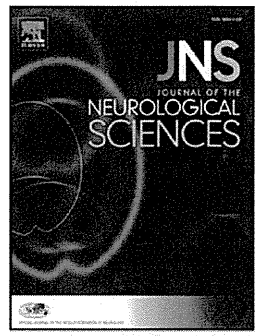

Congenital fiber type disproportion myopathy caused by *LMNA* mutations

Sachiko Kajino, Kayo Ishihara, Kanako Goto, Keiko Ishigaki, Satoru Noguchi, Ikuya Nonaka, Makiko Osawa, Ichizo Nishino, Yukiko K. Hayashi

PII: S0022-510X(14)00141-5
DOI: doi: 10.1016/j.jns.2014.02.036
Reference: JNS 13075

To appear in: *Journal of the Neurological Sciences*

Received date: 5 December 2013
Revised date: 24 February 2014
Accepted date: 26 February 2014

Please cite this article as: Kajino Sachiko, Ishihara Kayo, Goto Kanako, Ishigaki Keiko, Noguchi Satoru, Nonaka Ikuya, Osawa Makiko, Nishino Ichizo, Hayashi Yukiko K., Congenital fiber type disproportion myopathy caused by *LMNA* mutations, *Journal of the Neurological Sciences* (2014), doi: 10.1016/j.jns.2014.02.036

Congenital fiber type disproportion myopathy caused by *LMNA* mutations

Sachiko Kajino [a,b], Kayo Ishihara [a], Kanako Goto [a], Keiko Ishigaki [b], Satoru Noguchi [a,c], Ikuya Nonaka [a], Makiko Osawa [b], Ichizo Nishino [a,c], and Yukiko K Hayashi [a,c,d]

a. Department of Neuromuscular Research, National Institute of Neuroscience, National Center of Neurology and Psychiatry, Tokyo, Japan

b. Department of Pediatrics, Tokyo Women's Medical University, School of Medicine, Tokyo, Japan

c. Department of Clinical Development, Translational Medical Center, National Center of Neurology and Psychiatry, Tokyo, Japan

d. Department of Neurophysiology, Tokyo Medical University, Tokyo, Japan

Corresponding author; Yukiko K. Hayashi, MD, PhD

Mailing address: Department of Neurophysiology Tokyo Medical University, 6-1-1 Shinjuku, Shinjuku-ku, Tokyo 160-8402, JAPAN

Tel.:+81-3-3351-6141, Fax:+81-3-3351-6544

E-mail: yhayashi@tokyo-med.ac.jp

Keywords: LMNA-myopathy, CFTD, fiber type disproportion (FTD), *ACTA1*, *TPM3*, muscular dystrophy, congenital myopathy

Abstract

A boy, who had shown muscle weakness and hypotonia from early childhood and fiber type disproportion (FTD) with no dystrophic changes on muscle biopsy, was initially diagnosed as having congenital fiber type disproportion (CFTD). Subsequently, he developed cardiac conduction blocks. We reconsidered the diagnosis as possible LMNA-myopathy and found a heterozygous mutation in the *LMNA* gene. This encouraged us to search for *LMNA* mutations on 80 patients who met the diagnostic criteria of CFTD with unknown cause. Two patients including the above index case had heterozygous in-frame deletion mutations of c.367_369delAAG and c.99_101delGGA in *LMNA,* respectively. Four of 23 muscular dystrophy patients with *LMNA* mutation also showed fiber type disproportion (FTD). Importantly, all FTD associated with LMNA-myopathy were caused by hypertrophy of type 2 fibers as compared with age-matched controls, whereas CFTD with mutations in *ACTA1* or *TPM3* showed selective type 1 fiber atrophy but no type 2 fiber hypertrophy. Although FTD is not a constant pathological feature of LMNA-myopathy, we should consider the possibility of LMNA-myopathy whenever a diagnosis of CFTD is made and take steps to prevent cardiac insufficiency.

1. Introduction

Mutations in the gene encoding nuclear envelope proteins of A-type lamins (*LMNA*) cause several disorders referred to as laminopathies, which include skeletal and cardiac muscle disorders, lipodystrophy, peripheral neuropathy, and premature aging syndromes. Laminopathies predominantly affecting skeletal muscles (LMNA-myopathy) are clinically classified into three different phenotypes; Emery-Dreifuss muscular dystrophy (AD-, AR-EDMD), limb girdle muscular dystrophy type 1B (LGMD1B), and LMNA-related congenital muscular dystrophy (L-CMD). EDMD has distinctive clinical features including early joint contractures, humero-peroneal muscle weakness and dilated cardiomyopathy with conduction defects. LGMD1B is characterized by proximal muscle involvement and cardiomyopathy with conduction defects, but joint contracture is not prominent. L-CMD is an early onset form showing severe weakness of respiratory and neck muscles from infancy. Serum CK levels in LMNA-myopathy are normal to moderately elevated (2-20 times the upper limit of the normal range). Cardiac involvement, such as conduction blocks, dilated cardiomyopathy and sudden death, usually appears after the second decade of life. To minimize the risk of sudden cardiac death, early diagnosis and appropriate cardiac defibrillator implantation is recommended [1, 2, 3].

Pathologically, LMNA-myopathy is usually characterized by nonspecific dystrophic changes with variation in fiber size, mild necrotic and regenerating processes, and an

increased number of muscle fibers with internalized nuclei. Both type 1 and type 2 fibers are affected. Nuclear abnormalities are common [4]. Interestingly, marked mononuclear cellular infiltrations mimicking inflammatory myopathy can be seen in some patients with the infantile onset form of LMNA-myopathy [5].

We recently experienced a patient with a *LMNA* mutation whose initial diagnosis was congenital fiber type disproportion (CFTD). This patient had shown muscle weakness, hypotonia, and unstable gait from early childhood with no dystrophic changes, but prominent fiber type disproportion (FTD) on his muscle biopsy performed at 4 years of age. At his age of 16 years, he was pointed out to have atrial-ventricular conduction block and incomplete right bundle branch block. We thus reconsidered a possible diagnosis of LMNA-myopathy and identified a mutation in the *LMNA* gene.

CFTD is one of the congenital myopathies pathologically defined by smaller type 1 fibers, by at least 12%, than type 2 fibers without structural abnormalities such as nemaline bodies, cores, and central nuclei. Clinically, CFTD patients show generalized muscle hypotonia and weakness from infancy, multiple joint contractures, scoliosis, long thin face, and high arched palate. Approximately 30% of individuals with CFTD have mild-to-severe respiratory involvement. Cardiac involvement is seen in less than 10% of affected individuals [6, 7]. Six causative genes for CFTD have been identified: *ACTA1* [8], *TPM3* [9], *RYR1* [10], *TPM2* [11], *MYH7* [12] and *SEPN1* [13] encoding α-skeletal actin, α-tropomyosin slow, ryanodine receptor type 1, ß-tropomyosin, slow

β-myosin heavy chain and selenoprotein N1, respectively.

In this study, we genetically screened CFTD patients for mutations in *LMNA*. We also re-evaluated clinical and pathological findings in patients previously diagnosed as having LMNA-myopathy to ascertain whether these patients have features similar to those of CFTD.

2. Materials and methods

All clinical materials used in this study were obtained for diagnostic purposes with written informed consent. This work was approved by the Ethics Committee of the National Center of Neurology and Psychiatry (NCNP).

2.1. Patients

We examined 80 unrelated muscle biopsies from the NCNP muscle repository. All specimens were from patients who had been diagnosed as having CFTD based on pathological findings as well as clinical features. All cases satisfied the pathological criteria for CFTD; mean type 1 fiber diameter is at least 12% smaller than the mean type 2 fiber diameter, with no structural abnormalities such as nemaline bodies, cores, and increased number of fibers with internal nuclei. In addition, we re-evaluated muscle pathology findings from 23 unrelated patients who had previously been diagnosed as having LMNA-myopathy. We chose genetically confirmed CFTD patients

including 7 with *ACTA1* mutation and 2 with *TPM3* mutation for comparison of clinicopathological features. Clinically, all of the patients including in this study had muscle weakness and/or hypotonia from the preschool years (onset age; <6 years).

2.2 Mutation analysis

Genomic DNA was extracted from peripheral lymphocytes or frozen muscle specimens using standard techniques. For mutation screening of *LMNA*, *ACTA1* and *TPM3*, all exons and their flanking intronic regions were amplified by PCR and directly sequenced using an ABI PRISM 3100 automated sequencer (PE Applied Biosystems, Foster City, CA). Primer sequences are available on request.

2.3 Histochemical analysis of biopsied muscles

Biopsied skeletal muscles were frozen with isopentane cooled in liquid nitrogen. Serial frozen sections, 10 μm in thickness, were stained employing histochemical methods including hematoxylin and eosin (H&E), modified Gomori-trichrome (mGT), NADH-tetrazolium reductase (NADH-TR), and ATPases (pH 10.6, pH 4.6 and pH 4.3). For each muscle specimen, the mean fiber diameter was calculated by obtaining the shortest anteroposterior diameters of 100 type 1 and type 2 (A+B) fibers each using ATPase stains. Fiber size disproportion (FSD) was computed as; difference between type 2 fiber diameter (mean) and type 1 fiber diameter (mean) divided by type 2 fiber

diameter (mean) × 100%. To obtain muscle fiber size information for age-matched controls, a total of 18 muscle specimens with minimal pathological changes from each age were examined.

2.4. Electron microscopic observation

Muscle specimens were fixed with 2% glutaraldehyde in 0.1 M cacodylate buffer. After shaking with a mixture of 4% osmium tetroxide, 1.5% lanthanum nitrate, and 0.2 M s-collidine for 2-3 h, samples were embedded in epoxy resin. Semi-thin sections (1 μm-thickness) were stained with toluidine blue. Ultrathin sections, 50 nm in thickness, were stained with uranyl acetate and lead citrate, and then examined under a tecnai spirit transmission electron microscope (FEI, Japan) at 120 kV.

2.5. Statistical analysis

All data are presented as means ± SD. Comparisons among groups were made using Student's *t* test and analysis of variance (ANOVA). A difference was considered to be statistically significant at a p value less than 0.05.

3. Results

3.1 Mutation analysis

Among the 80 unrelated patients who were diagnosed as having CFTD based on

clinical and pathological findings, a heterozygous *LMNA* mutation was identified in two; a previously reported c.367_369delAAG (p.Lys123del) in Patient 1 and a novel c.99_101delGGA (p.Glu33del) in Patient 2 [14]. *ACTA1* mutations found in the 7 CFTD patients were c.16G>A (p.Glu6Lys), c.142G>T (p.Gly48Cys), c.668T>C (p.Leu223Pro), c.682G>C (p.Glu228Gln), c.981T>A (p.Met326Lys), and c.1000C>T (p.Pro334Ser). Two CFTD patients had the same heterozygous c.502C>T (p.Arg168Cys) mutation in *TPM3.* The novel mutations of *LMNA* c.99_101delGGA (p.Glu33del) and *ACTA1* c.981T>A (p.Met326Lys), were not found in either 100 Japanese control chromosomes or the dbSNP and 1000 Genomes databases.

3.2 Histological findings

Histologically, type 1 fiber predominance (more than 55% of type 1 fibers) and type 2B fiber deficiency (less than 5% of type 2B fibers) were observed in 61% and 28%, respectively, of our 80 CFTD cohort. These results are consistent with those of a previous report [7].

Two patients with *LMNA* mutations showed a marked difference in the sizes of type 1 and type 2 fibers, resulting in FSD of 57% and 13%, respectively (Figure 1). Neither type 1 fiber predominance nor type 2B fiber deficiency was seen (Table 1).

Re-evaluation of genetically confirmed LMNA-myopathy revealed that 4 of 23 patients (17%) had fiber type disproportion (FTD). Their FSD was ranged from 15 to

42%. All 4 patients with FTD also showed some necrotic and/or regenerating fibers in their muscle biopsy and had a diagnosed of muscular dystrophy. These 4 patients with FTD had 3 different mutations. Two mutations of c.1583C>A (p.Thr528Lys) and c.1357C>T (p.Arg453Trp) have already been reported [15, 16], whereas the c.907T>C (p.Ser303Pro) mutation was not reported previously. These mutations were distributed in both central rod and tail domains, but not in the head domain (Table 1).

To clarify whether LMNA-myopathy patients with FTD have specific pathological findings different from those affecting CFTD muscles with known gene mutations, we carefully re-evaluated the muscle pathologies of the 6 LMNA-myopathy patients with FTD, 7 CFTD patients with *ACTA1* mutations, and 2 CFTD patients with *TPM3* mutations. FSD in LMNA-myopathy with FTD, and in CFTD with *ACTA1* and *TPM3* mutations were calculated to be 27.8 ± 17.9% (mean ± SD), 37.7 ± 12.1%, and 54.1 ± 13.1%, respectively. No significant differences were seen in FSD among the 3 groups. We also compared fiber sizes among LMNA-myopathy with FTD, CFTD with *ACTA1* or *TPM3* mutations and age-matched controls. Surprisingly, CFTD with *ACTA1* and *TPM3* mutations showed type 1 fiber atrophy, whereas LMNA-myopathy with FTD showed type 2 fiber hypertrophy with lack of type 1 fiber atrophy (Figure 2).

In this study, type 1 fiber predominance was seen in 86% of CFTD patients with *ACTA1* mutations and in 100% of those with *TPM3* mutations, but in only 33% of LMNA-myopathy patients with FTD. The percentage of type 1 fibers in

LMNA-myopathy was calculated to be 44.6 ± 12.8 (mean ± SD), which was significantly lower than that in CFTD with *ACTA1* mutations (64.1 ± 7.1%) and that with *TPM3* mutations (57.0 ± 1.4%) ($p < 0.05$). Type 2B fiber deficiency was not seen in LMNA-myopathy with FTD (Table 1, 3), whereas 4 of 7 (57%) patients with *ACTA1* mutations and one (50%) with *TPM3* mutation showed type 2B fiber deficiency.

On electron microscopic (EM) observations, nuclear changes are important pathological findings in skeletal muscles of LMNA-myopathy [4]. We examined the nuclear changes in Patients 2, 4 and 5 on EM, and found a few myonuclei showing abnormal shapes and chromatin disorganization (Figure 3). Smaller nuclei arranged in a row, giving the appearance of a 'nuclear chain', were also seen (data not shown). However, nuclear abnormalities in patients who had LMNA-myopathy with FTD were milder and less frequent than previously reported for AD-EDMD and LGMD1B muscles [4].

3.3 Clinical findings

Table 2 summarizes the characteristics of the 6 LMNA-myopathy patients with FTD. Patients 1 and 2 were initially diagnosed as having CFTD, and the 4 remaining patients (patients 3 to 6) showed FTD together with dystrophic changes on muscle pathology. All patients had normal antenatal courses and uneventful births. All patients had started walking without delay, but showed a waddling gait and muscle

weakness and/or hypotonia from the preschool years. None had a high arched palate or respiratory dysfunction. Four of the 6 (67%) patients had contractures of the ankles and/or elbows which had not been present at birth but appeared with age. Serum creatine kinase (CK) was mildly elevated in all patients.

Sixteen of the 78 (21%) CFTD patients with unknown cause had high CK levels (>200 IU/l), and four of these 16 showed a high arched palate and respiratory involvement.

4. Discussion

FTD can be seen in a single muscle biopsy from patients with several diseases including congenital myotonic dystrophy and centronuclear myopathy [17-20]. Here we identified 2 LMNA-myopathy among patients diagnosed as CFTD. We also found FTD in 17% of muscular dystrophy patients with LMNA mutations. These results suggest that FTD may not be rare in LMNA-myopathy. None of these patients had either a high arched palate or respiratory insufficiency, and serum CK levels were mildly elevated. Pathologically, FTD in LMNA-myopathy is associated with type 2 fiber hypertrophy with lack of type 1 fiber atrophy, whereas type 1 fiber atrophy is seen in CFTD with *ACTA1* or *TPM3* mutations. Unlike CFTD due to *ACTA1* or *TPM3* mutations, type 1 fiber predominance and type 2B fiber deficiency are absent in LMNA-myopathy. These results suggest that *LMNA* analysis should be performed in CFTD patients who has the clinical features such as no high arched palate, no respiratory insufficiency and